DOI: 10.1002/ejic.201100349

Synthesis and Thermal Stability Studies of $CaFe_4As_3$

Tanghong Yi,[a] Adam P. Dioguardi,[b] Peter Klavins,[b] Nicholas J. Curro,[b] Liang L. Zhao,[c] E. Morosan,[c] and Susan M. Kauzlarich*[a]

Dedicated to Professor John D. Corbett on the occasion of his 85th birthday

Keywords: Calcium / Iron / Arsenic / Superconductors / Intermetallic phases / Solid-state reactions / Thermal stability

$CaFe_4As_3$ is a new intermetallic structure type that can be described as a framework comprising of $FeAs_4$ tetrahedra. The structure has similarities to the 1-2-2 superconducting phase in that the Fe/As network is related to the $ThCr_2Si_2$ structure. In addition, this phase shows magnetic transitions associated with spin density waves. This phase was prepared from a Sn flux, and it has recently been reported that further expansion of this structure type via chemical substitution is limited. We have developed a solid-state synthesis route for the preparation of $CaFe_4As_3$ that involves reacting a stoichiometric combination of the constituent elements. The thermal stability of this material was investigated over the 298–1473 K temperature range. An initial investigation of the Sn grown $CaFe_4As_3$ crystals showed that residual Sn that was present on the surface of the crystals reacted with the crystals at temperatures above 1173 K to form new phases. A thermal stability study of Sn-free $CaFe_4As_3$ indicated that it decomposed to give $CaFe_2As_2$ and Fe_2As. The thermal behavior of $CaFe_2As_2$ was also investigated and the data showed that it can also form $CaFe_4As_3$ at high temperatures. The solid-state synthesis route presented herein and additional solid solution studies may provide opportunities for the prepartion of materials with this structure type with improved electronic properties.

Introduction

The recent discovery of the unconventional iron-based layered superconductors $La[O_{1-x}F_x]FeAs$ opened a new chapter in superconductivity.[1] Extensive research concerned with understanding the mechanism responsible for the superconductivity in this family of materials has included the synthesis of new compounds containing FeAs layers. $CaFe_4As_3$ is one of the new iron pnictide compounds that has been discovered.[2] Although it does not show superconductivity above 1.8 K, its structure and complex electronic and magnetic properties make $CaFe_4As_3$ an attractive compound to study.[2b] $CaFe_4As_3$ crystallizes in the orthorhombic space group *Pnma*. Figure 1 shows a view of the crystal structure. Unlike other compounds with FeAs layers, $CaFe_4As_3$ has infinite $Fe^{II}{}_2As_2$ layers that are stacked along the direction of the *b*-axis and finite Fe_2As_2 layers that are stacked in directions perpendicular to the *b*-axis. Five-coordinated Fe^{I} ions and additional four-coordinated Fe^{II} ions interconnect with the infinite Fe_2As_2 layers to form a 3D covalent network with ribbons that lie in the *ac*-plane.[2b] AFe_2As_2 (A = alkali earth metal) compounds display first order structural phase transitions when converting from high temperature tetrahedral to low temperature orthorhombic structures.[3] $CaFe_4As_3$ undergoes two magnetic transitions at approximately 88 K and 26 K, respectively. The first transition at below 88 K is attributed to a second order phase transition with an incommensurate spin-density wave ordering that occurs along the *b*-axis of the structure. The second transition is described as a first order transition from an incommensurate to commensurate

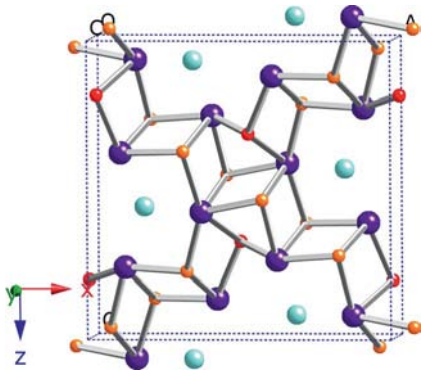

Figure 1. A view of the $CaFe_4As_3$ structure projected along the *b*-axis. The Ca, As, four-coordinated Fe^{II}, and five-coordinated Fe^{I} ions are represented by blue, purple, yellow, and red spheres, respectively.

[a] Department of Chemistry, University of California Davis, One Shields Avenue, Davis, California 95616, USA
Fax: +1-530-752-8995
E-mail: smkauzlarich@ucdavis.edu
[b] Department of Physics, University of California Davis, One Shields Avenue, Davis, California 95616, USA
[c] Department of Physics and Astronomy, Rice University, Houston, Texas 77005, USA

state.[4] The transition at 88 K is clearly reflected in the specific heat capacity data for $CaFe_4As_3$, and the transition at 26 K causes an abrupt reduction in the material's electrical resistivity at this temperature.[2] However, no structural changes such as those that occur in AFe_2As_2 layered compounds were observed for $CaFe_4As_3$.

Recently, the substitution of Ca, Fe, or As with various dopants has been attempted by flux reactions in order to modify the anisotropic magnetic structure of $CaFe_4As_3$.[5] However, this method only succeeded in partially replacing the five-coordinated Fe^{I} ions in $CaFe_4As_3$ with Cr.

In the current paper, we focus on the problems associated with the Sn flux synthesis of $CaFe_4As_3$ single crystals that were revealed by differential scanning calorimetry (DSC) measurements, and present a new synthetic method to obtain this compound that may also allow for structural analogs of $CaFe_4As_3$ to be prepared. A detailed study conducted over the 298–1473 K temperature range of the thermal stabilities of $CaFe_4As_3$ single crystals prepared by Sn flux and polycrystals prepared by the direct reaction of the constituent elements is also reported, and this information allows for a better understanding of the complexities of the synthetic procedure.

Results and Discussion

Synthesis and X-ray Characterization

The recently synthesized compound $CaFe_4As_3$ was discovered serendipitiously as a side product in the reaction designed to prepare $CaFe_2As_2$ via a Sn flux route.[2] The reaction parameters were optimized to grow large $CaFe_4As_3$ crystals in high yield.[2b] The details of this synthesis have been reported elsewhere.[2b] Microprobe analysis was performed on $CaFe_4As_3$ single crystals. Needle-shaped crystals were formed in the flux reaction, as shown in the back scattering electron (BSE) image of the reaction product (Figure 2, see inset a). The white droplets on the surface of crystals in the BSE image are residual Sn flux. Centrifugation is the preferred method employed to separate the crystals from the Sn flux. One drawback of the flux reaction is that it can be difficult to completely remove the flux from the reaction products. Typically, the flux is removed via high temperature centrifugation. This requires practice, and if the temperature is too low it is difficult to remove all the Sn. However, regardless of the temperature or the speed of centrifugation, small droplets of residual Sn were always found on the surface of the $CaFe_4As_3$ crystals. Acid etching may be a viable option for removing the flux, but in many cases the crystals are also sensitive to the acid.[6] A representative area of a $CaFe_4As_3$ crystal was chosen for X-ray element mapping. The element maps showed that all the elements, Ca, Fe and As, were homogeneously distributed over the crystal surface (Figure 2, b–d). Quantitative analysis by wavelength dispersive X-ray spectroscopy (WDS) gave a composition of $Ca_{1.00(1)}Fe_{4.07(4)}As_{3.05(5)}$ for the major phase of the product. The data obtained from a microprobe analysis are in good agreement with the result from a single crystal diffraction analysis of the $CaFe_4As_3$ product.

Phase pure $CaFe_4As_3$ can also be obtained by directly reacting stoichiometric amounts of the constituent elements and annealing at 1173 K. A powder X-ray diffraction pattern of polycrystalline $CaFe_4As_3$ prepared from this solid-state method is compared in Figure 3 with powder X-ray diffraction data for ground single-crystals and a simulated pattern for $CaFe_4As_3$. These XRD patterns show the high quality of the polycrystalline $CaFe_4As_3$ obtained from the stoichiometric reaction. The room temperature lattice parameters determined from the refinement, performed with

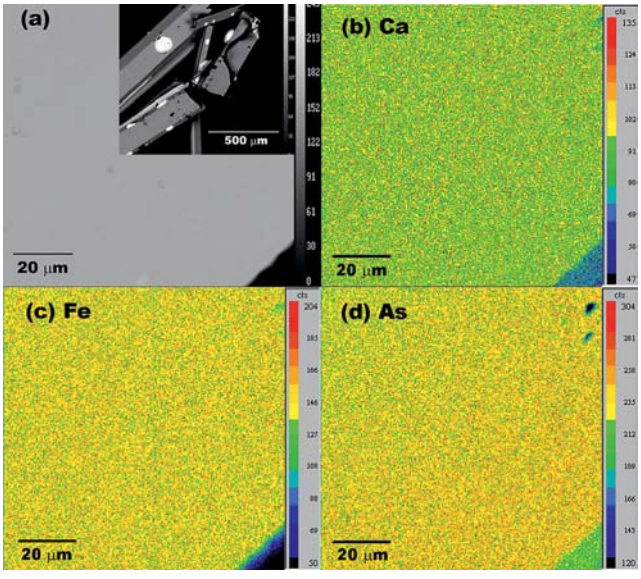

Figure 2. (a) BSE image of a representative clean area of the $CaFe_4As_3$ single crystals. The inset shows a BSE image of the needle shaped $CaFe_4As_3$ single crystals; (b) X-ray element map of Ca; (c) X-ray element map of Fe; (d) X-ray element map of As. As shown in by the scale bar the relative intensities for the element maps increase from black to white/red.

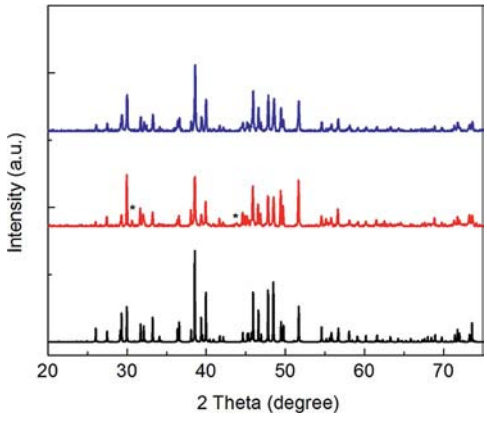

Figure 3. Powder XRD pattern of polycrystalline $CaFe_4As_3$ obtained from a solid-state reaction (blue) compared with data for ground single crystals (red), and a simulated pattern for $CaFe_4As_3$ (black). The simulated pattern was calculated from a cif file (90 K[2b]) with room temperature lattice parameters a = 11.9108(4) Å, b = 3.7466(2) Å, c = 11.6178(5) Å. (*: Sn).

the Jade 6 software,[7] of the XRD data for the polycrystalline sample of $CaFe_4As_3$ are: a = 11.9101(10) Å, b = 3.7465(3) Å, c = 11.6164(9) Å, and V = 518.34 Å^3. These values are similar, i.e. within standard deviation, to those determined from the data for the ground single crystals: a = 11.9108(4) Å, b = 3.7466(2) Å, c = 11.6178(5) Å, V = 518.44 Å^3. The unit cell volume determined for polycrystalline $CaFe_4As_3$ is slightly larger (by ca. 0.27%) than the room temperature value reported by Todorov et al. for single crystals of this material,[2a] but is consistent with the reported value obtained at lower temperature.[2] Signals arising from residual Sn flux (marked by asterisks) appear in the diffraction pattern of the ground single crystal sample. The higher than expected intensity of the indexed peaks for reflections (400), (504) and (406), at 2θ values of approximately 30°, 49.4° and 56.6°, respectively, is attributed to the preferred orientation the crystallites.

Thermal Stability

Thermogravimetry-differential scanning calorimetry (TG-DSC) was employed to investigate the thermal stability of $CaFe_4As_3$. The single crystals produced from the flux reaction have complex DSC curves, which are shown in Figure 4. The highest temperature, 1473 K, employed in this study was chosen as it was noted that the $CaFe_4As_3$ single crystals did not change morphology when heated to only 1273 K, and only visually exhibited indications of melting behavior after being heated to 1473 K. The curve corresponding to the first heating cycle showed a small endotherm at approximately 505 K, along with a number of small endotherms above 1000 K. The endothermic peak in the DSC heating curve at around 505 K was assigned to the melting of the residual Sn flux that was present on the surface of the $CaFe_4As_3$ crystals. It was expected that an exothermic peak at around 505 K would present in the curve for the first cooling process, which would correspond to the recrystallization or solidification of the Sn. However, no recrystallization peak was apparent in the curves for either cycle. This indicated that the residual Sn reacted with the $CaFe_4As_3$, or its derivative compounds, at high temperatures. The exotherms in the curve for the first cooling process occurred at approximately 792 K, 1013 K, 1179 K, 1230 K, and 1273 K, indicative of the occurrence of chemical transformations, solidification or crystallization processes. A second heating/cooling cycle was run in order to confirm the occurrence of the melting/crystallization processes. The melting peak for Sn that is expected at ca. 505 K is not present in the heating curve of the second cycle, while a number of new endotherms were seen in the curve at approximately 809 K, 1043 K, 1158 K, 1230 K, and 1296 K. The new endothermic peaks are assigned to the melting or chemical transformations of the phases that formed during the first heating/cooling cycle. All the exotherms seen in the second cooling curve matched well with those observed in the first cooling curve, which confirmed that the phases were prepared during the first heating process. X-ray powder diffraction data were taken of the solid after the second cycle, and these are shown in Figure 5. Peaks associated with ternary phases $CaFe_4As_3$, $CaFe_2As_2$, and binary phases Fe_2As, FeAs and $FeSn_2$ can be indexed in the XRD pattern.

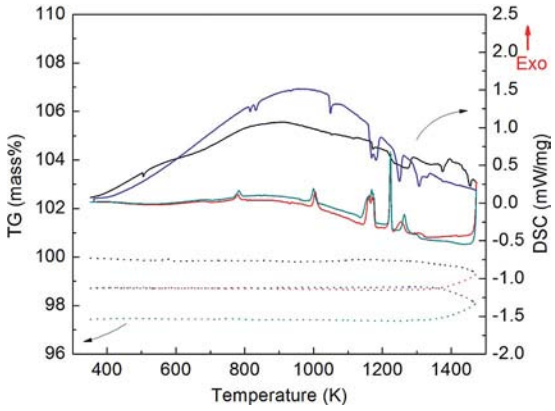

Figure 4. TG-DSC analysis of $CaFe_4As_3$ single crystals. The solid lines are DSC curves, and the dotted lines are TG curves. The black, red, blue and green lines correspond to 1st heating, 1st cooling, 2nd heating, and 2nd cooling processes, respectively.

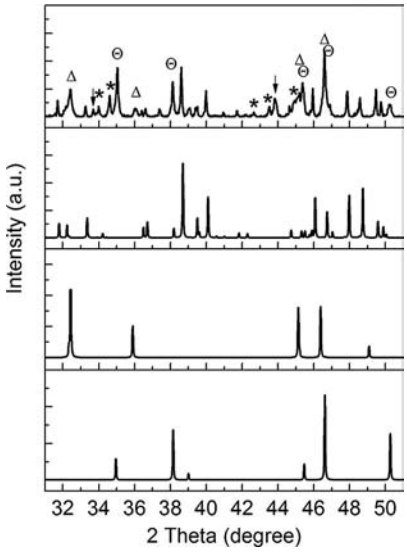

Figure 5. XRD pattern of $CaFe_4As_3$ single crystals recorded after they were subject to TG-DSC analysis and heated up to 1473 K (top) compared with simulated patterns for $CaFe_4As_3$ (2nd from top), tetragonal $CaFe_2As_2$[8] (3rd from top) and Fe_2As[9] (bottom) phases. The peaks contributed by minor phases to the experimental XRD pattern are indicated by different symbols (Δ: tetragonal $CaFe_2As_2$; Θ: Fe_2As; *: AsFe; arrow: $FeSn_2$).

In order to investigate in more detail of the thermal stability of the compound $CaFe_4As_3$, and to determine the effect of Sn on the type of product produced by heating this material, a polycrystalline sample of $CaFe_4As_3$ was prepared via a solid-state reaction and its thermal stability was measured. For the purposes of comparison, the same programming profile that was used for the TG-DSC analysis of the single crystals was employed for the analysis of this polycrystalline sample. Simpler DSC curves were obtained

for the polycrystalline sample relative to those for the single crystals, and these are shown in Figure 6. The endothermic and exothermic peaks in the heating and cooling DSC curves for both cycles recorded for the polycrystalline sample matched, with the exception of the first endothermic peak at approximately 1110 K in the second heating curve, which barely registered in the first heating curve. Three pairs of endothermic and exothermic peaks are revealed at approximately 1110, 1253, and 1313 K in the heating and cooling DSC curves of the second cycle. The presence of these corresponding pairs indicated that three reversible phase transitions took place. The phases produced from the $CaFe_4As_3$ polycrystalline sample during the TG-DSC measurements were identified by XRD as a mixture of $CaFe_4As_3$, $CaFe_2As_2$ and Fe_2As, the XRD pattern is shown in Figure 7.

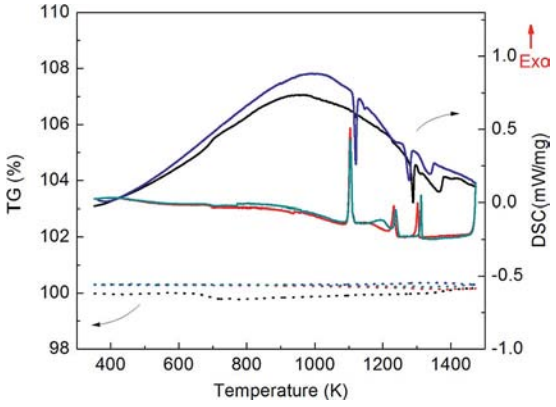

Figure 6. TG-DSC curves for polycrystalline $CaFe_4As_3$ produced from a solid-state reaction. The solid lines are DSC curves, and the dotted lines are TG curves. The black, red, blue and green lines correspond to 1st heating, 1st cooling, 2nd heating, and 2nd cooling processes, respectively.

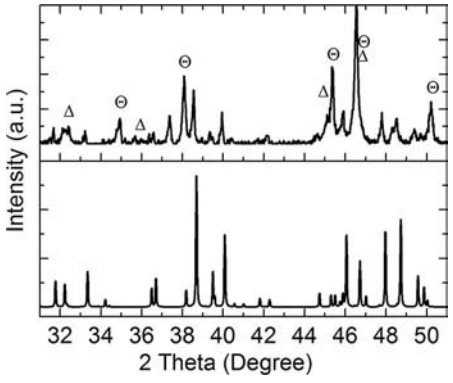

Figure 7. XRD pattern of polycrystalline $CaFe_4As_3$ produced from a solid-state reaction recorded after the material was subject to TG-DSC analysis and heated up to 1473 K (top) compared with a simulated pattern for $CaFe_4As_3$ (bottom). The peaks contributed by minor phases to the experimental XRD pattern are indicated by different symbols (Δ: tetragonal $CaFe_2As_2$; Θ: Fe_2As).

Without the effect of Sn, $CaFe_4As_3$ decomposed at high temperature to give $CaFe_2As_2$ and Fe_2As according to the balanced reaction equation: $CaFe_4As_3 \rightarrow CaFe_2As_2 + Fe_2As$. By measuring powder XRD patterns of the samples after the TG-DSC heating cycle, we were able to assign the three pairs of peaks in the DSC curves, Figure 6, to the melting and recrystallization of Fe_2As (1110 K), $CaFe_2As_2$ (1253 K) and $CaFe_4As_3$ (1313 K). These assignments were further confirmed by TG-DSC analyses of $CaFe_4As_3$, $CaFe_2As_2$ and Fe_2As samples conducted at different temperatures. The morphology of the $CaFe_4As_3$ crystals remained unchanged below 1273 K, but the crystals completely melted after being heated to 1473 K. This indicated that $CaFe_4As_3$ melted at a temperature between 1273 K and 1473 K. The same experimental strategy was used to confirm the melting of $CaFe_2As_2$ crystals between 1173 K and 1273 K. The TG-DSC curve of a polycrystalline sample of Fe_2As showed a clear melting process occurring at 1113 K, as shown in Figure 8. This melting point for Fe_2As is at a slightly lower temperature than a previously reported value of 1192 K.[10] This melting point depression is attributed to the presence of other phases in the sample mixture. For example, Fe_2As can melt at a much lower temperature than expected when Cu is present as an impurity.[11] The melting peak of Fe_2As was discernible in the heating curve for the first cycle recorded with polycrystalline $CaFe_4As_3$ (Figure 6), while it grew in intensity in the heating curve for the second cycle. This indicated that the decomposition reaction that happens above 1173 K produces more Fe_2As.

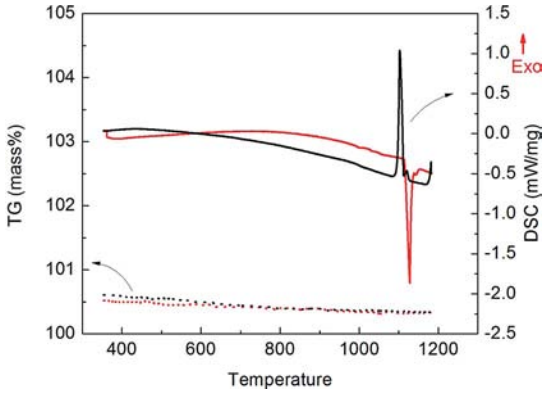

Figure 8. TG-DSC data recorded up to 1183 K for a polycrystalline Fe_2As sample. The solid lines are DSC curves, and the dotted lines are TG curves. The red and black curves correspond to heating and cooling processes, respectively.

A similar thermal stability study was performed on $CaFe_2As_2$ since a mixture of $CaFe_4As_3$ and $CaFe_2As_2$ was prepared from the flux reaction. A TG-DSC measurement was performed on the tetragonal $CaFe_2As_2$ single crystals that had a plate shape; however, these data not shown herein. Peaks corresponding to the melting and crystallization of Sn were observed in the DSC curves when the sample was heated up to 1173 K. No additional phases were observed in the XRD pattern that were recorded after the single crystals were heated up to 1173 K during the two TG-DSC cycles. However, $CaFe_4As_3$ and Fe_2As, as well as $CaFe_2As_2$, were observed in the XRD pattern of the $CaFe_2As_2$ single crystal that was recorded after the crystal was exposed to two TG-DSC cycles and heated up to 1473 K, as shown in Figure 9. The analysis suggested that

the following reaction had taken place: $3CaFe_2As_2 \rightarrow CaFe_4As_3 + Fe_2As + 2As + 2Ca$. Calcium may react to form amorphous Ca-Sn binary phases or CaO. Sn also may participate in this reaction, which would result in a more complex chemical equation. A slight weight gain was observed when the crystals were heated below 1273 K, which is consistent with oxidation of the elements. The $CaFe_2As_2$ crystals displayed an approximate 3.5% weight loss after being heated to1473 K during the two TG-DSC cycles. This slight weight loss may be indicative of sublimation of the As. The process of oxidation and sublimation of As (As^{3-} to As^0) could provide electrons to reduce some of the Fe^{II} (in $CaFe_2As_2$) to Fe^{I} (in $CaFe_4As_3$).

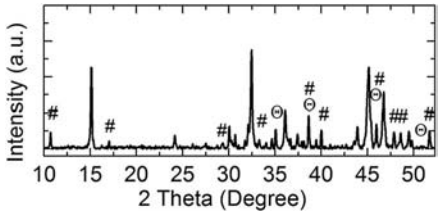

Figure 9. XRD pattern of $CaFe_2As_2$ single crystals recorded after they were subjected to TG-DSC analysis and heated to 1473 K. The peaks contributed by minor phases to the experimental XRD pattern are indicated by different symbols (#: $CaFe_4As_3$; Θ: Fe_2As).

Conclusions

$CaFe_4As_3$ was synthesized from direct reaction of the constituent elements that were sealed in Nb tubes. $CaFe_4As_3$ decomposes at a temperature above 1173 K to give $CaFe_2As_2$ and Fe_2As. Compound $CaFe_2As_2$ can also convert to $CaFe_4As_3$. Residual Sn flux present on the surface of $CaFe_4As_3$ and $CaFe_2As_2$ crystals grown by a flux method can react with the crystals at temperatures above 1173 K to generate binary phases. This thermal stability study is valuable for aiding in the fabrication of pure $CaFe_4As_3$ and for further expanding the number of compounds with this structure type,[5] thereby allowing further structure-property investigations to be conducted with aim of tuning the magnetic and electronic properties of this class of compound.

Experimental Section

Synthesis: Pure phase $CaFe_4As_3$ was obtained from a solid-state reaction. Stoichiometric amounts of the constituent elements, Ca (Aldrich, dendritic pieces, 99.99%) Fe (Aldrich, granules 10–30 mesh, 99.999%), and As (Johnson Matthey Chemicals, lump), were loaded in to an Nb tube that was 5 cm long and 1 cm in diameter, the tube was then sealed with an Argon arc welder. The sealed Nb tube was then sealed in an evacuated fused silica tube. The reaction vessel was placed in a programmable furnace and heated to 1173 K over a period of 6 h before being held at 1173 K for one week. Silver-colored pieces of $CaFe_4As_3$ were obtained after the Nb tube was opened in air. $CaFe_4As_3$ and $CaFe_2As_2$ single crystals were synthesized from Sn flux following a processes reported in the literature.[2b,3b,3e] Polycrystalline Fe_2As was prepared by a solid-state reaction. A mixture of Fe and As in the desired ratio was loaded in to a fused Nb tube that was then sealed in an evacuated quartz tube. This tube was placed in a programmable furnace and heated to 873 K over a 6 h period, then held at this temperature for a further 6 h before being heated to 1273 K over a 6 h period and held at this temperature for 24 h. The ampoule was finally cooled slowly to room temperature.

Powder X-ray Diffraction: Single crystals produced from a flux reaction or crystalline pieces from a solid-state reaction were ground into powers for powder X-ray diffraction (XRD) analyses. Room temperature XRD data were collected by a Bruker D8 diffractometer with Cu-K_α radiation (λ = 1.5406 Å). The data analysis, cell refinements, and whole pattern fitting refinements were performed with the MDI JADE 6.1 software.[7]

Microprobe Analysis: Microprobe measurements were performed on single crystals with a Camera SX-100 electron probe microanalyzer equipped with a wavelength-dispersive spectrometer. Samples were prepared by mounting the crystals onto 25 mm plastic rounds with epoxy and then carbon coating them to conduct charges. The surfaces were polished smooth prior to measurement. The compounds $CaMoO_4$, Fe_2O_3 and InAs were calibration standards for the quantitative analysis of Ca, Fe, and As, respectively. Each sample was scanned with a spot size of 1 μm and data were collected at 13 points on the crystal surface. The composition of the sample was calculated as an average of the data recorded at all points.

Thermogravimetry-Differential Scanning Calorimetry (TG-DSC): Crystals from a flux reaction, pieces from a solid-state reaction, and ground powder from crystals and pieces, were used for TG-DSC analyses. Data were collected by a Netzsch Thermal Analysis STA 409 cell equipped with a TASC 414/2 controller and PU 1.851.01 power unit. The sample was loaded into an alumina crucible at room temperature, and after purging the sample chamber data were collected with the sample kept under flowing argon (flow rate: 10 K/min). Data were recorded by the software provided with the equipment and analyzed with the Netzsch Proteus computer program.

Acknowledgments

This research was funded by National Science Foundation (NSF), DMR-0600742. The authors gratefully acknowledge Dr. Sarah Roeske and Brian Joy for the microprobe analysis.

[1] Y. Kamihara, T. Watanabe, M. Hirano, H. Hosono, *J. Am. Chem. Soc.* **2008**, *130*, 3296–3297.
[2] a) I. Todorov, D. Y. Chung, C. D. Malliakas, Q. A. Li, T. Bakas, A. Douvalis, G. Trimarchi, K. Gray, J. F. Mitchell, A. J. Freeman, M. G. Kanatzidis, *J. Am. Chem. Soc.* **2009**, *131*, 5405–5407; b) L. Zhao, T. Yi, J. C. Fettinger, S. M. Kauzlarich, E. Morosan, *Phys. Rev. B: Condens. Matter* **2009**, *80*, 020404.
[3] a) A. I. Goldman, D. N. Argyriou, B. Ouladdiaf, T. Chatterji, A. Kreyssig, S. Nandi, N. Ni, S. L. Bud'ko, P. C. Canfield, R. J. McQueeney, *Phys. Rev. B: Condens. Matter* **2008**, *78*, 100506; b) P. C. Canfield, S. L. Bud'ko, N. Ni, A. Kreyssig, A. I. Goldman, R. J. McQueeney, M. S. Torikachvili, D. N. Argyriou, G. Luke, W. Yu, *Physica C - Superconductivity and Its Applications* **2009**, *469*, 404–412; c) M. Rotter, M. Tegel, D. Johrendt, *Phys. Rev. B: Condens. Matter* **2008**, *78*, 020503; d) P. C. Canfield, S. L. Bud'ko, N. Ni, J. Q. Yan, A. Kracher, *Phys. Rev. B* **2009**, *80*, 060501; e) N. Ni, S. Nandi, A. Kreyssig, A. I. Goldman, E. D. Mun, S. L. Bud'ko, P. C. Canfield, *Phys. Rev. B* **2008**, *78*, 014523.
[4] a) P. Manuel, L. C. Chapon, I. S. Todorov, D. Y. Chung, J. P. Castellan, S. Rosenkranz, R. Osborn, P. Toledano, M. G. Kan-

atzidis, *arXiv.org, e-Print Arch., Condens. Matter* **2010**, 1–4; arXiv:1002.1336v1001 [cond-mat.str-el]; b) Y. Nambu, L. L. Zhao, E. Morosan, K. Kim, G. Kotliar, P. Zajdel, M. A. Green, W. Ratcliff, J. A. Rodriguez-Rivera, C. Broholm, *Phys. Rev. Lett.* **2011**, *106*, 037201.

[5] I. Todorov, D. Y. Chung, H. Claus, K. E. Gray, Q. A. Li, J. Schleuter, T. Bakas, A. P. Douvalis, M. Gutmann, M. G. Kanatzidis, *Chem. Mater.* **2010**, *22*, 4996–5002.

[6] a) A. B. Karki, G. T. McCandless, S. Stadler, Y. M. Xiong, J. Li, J. Y. Chan, R. Jin, *Submitted to Phys. Rev. B* **2011**; arXiv:1103.3852v1; b) P. C. Canfield, Z. Fisk, *Philos. Mag. B* **1992**, *65*, 1117–1123; c) T. Yi, C. A. Cox, E. S. Toberer, G. J. Snyder, S. M. Kauzlarich, *Chem. Mater.* **2010**, *22*, 935–941.

[7] MDI Materials Database Livermore, CA, **2003**.

[8] F. Ronning, T. Klimczuk, E. D. Bauer, H. Volz, J. D. Thompson, *J. Phys. Condens. Matter* **2008**, *20*, 322201.

[9] H. Katsurak, N. Achiwa, *J. Phys. Soc. Jpn.* **1966**, *21*, 2238–2243.

[10] M. Elander, G. Hagg, A. Westgren, *Ark. Kemi, Mineral. Geol.* **1936**, *12B*, 1–6.

[11] N. I. Kopylov, S. V. Degtyarev, N. P. Tolkachev, M. Z. Toguzov, Y. I. Chirik, *Russ. J. Inorg. Chem.* **1984**, *29*, 625–627.

Received: April 1, 2011
Published Online: August 10, 2011

